Complex networks for analyzing the urban acoustic environment

Timo Haselhoff[a]*, Tobias Braun[b], André Fiebig[c], Jonas Hornberg[a], Bryce T. Lawrence[d], Norbert Marwan[b], Susanne Moebus[a]

[a]Institute for Urban Public Health, University Hospital Essen, University Duisburg-Essen, 45147 Essen, Germany
[b]Complexity Science, Potsdam Institute for Climate Impact Research, Member of the Leibniz Association, 14473 Potsdam, Germany
[c]Engineering Acoustics, Technical University of Berlin, 10587 Berlin, Germany
[d]Department of Spatial Planning, TU Dortmund University, 44227 Dortmund, Germany
*Corresponding Author (E-Mail: timo.haselhoff@uk-essen.de)

Abstract

The urban acoustic environment (AE) provides comprehensive acoustic information related to the diverse systems of urban areas, such as traffic, the built environment, or biodiversity. The decreasing cost of acoustic sensors and rapid growth of storage space and computational power have fostered the collection of large amounts of acoustical data to be processed. However, despite the extensive information that is recorded by modern acoustic sensors, few approaches are established to capture the rich complex dynamics embedded in the time-frequency domain of the urban AE. Quantitative methods need to account for this complexity, while effectively reducing the high dimensionality of acoustic features within the data. Therefore, we introduce complex networks as a tool for analyzing the complex structure of large-scale urban AE data. We present a framework to construct networks based on frequency correlation matrices (FCMs). FCMs have shown to be a promising tool to depict environment specific interrelationships between consecutive power spectra. Accordingly, we show the capabilities of complex networks for the quantification of these interrelationships and thus, to characterize different urban AEs.

We demonstrate the scope of the proposed method, using one of the world's most extensive longitudinal audio datasets, considering 3-min audio recordings (n = 319,385 ≙ 665 days) from 23 sites. We construct networks from hour-of-day specific audio recordings for each site. We show that the average shortest path length (ASPL) as an indicator for dominance of sound sources in the urban AE exhibits spatial- and temporal-specific patterns between the sites, which allows us to identify four to seven clusters of distinct urban AEs. To validate our findings, we use the land use mix around each site as a proxy for the AE and compare those between and within the clusters. The identified clusters show high intra- and low inter-cluster correlations of ASPL diel cycles as well as strong intra-similarities in land use mix. Our results indicate that complex networks are a promising approach to analyze large-scale audio data, expanding our understanding of the time-frequency domain of the urban AE.

1 Introduction

The urban acoustic environment (AE) is a rich source of information. In soundscape ecology, the AE is monitored to access information about biodiversity, species abundance or to study the impacts of climate change (Farina, 2013; Kasten et al., 2012; Krause and Farina, 2016; Pijanowski et al., 2011; Sueur, 2018; Sueur and Farina, 2015). In urban planning, the AE is analyzed to, e.g. characterize and design public or private spaces (Botteldooren et al., 2013; De Coensel et al., 2010; Kang and Schulte-Fortkamp, 2016; Rehan, 2016). Common methods to analyze the urban AE include, e.g. the perceptual soundscape approach (DIN ISO 12913-1:2018-02). Here, individual ratings about the AE are used to evaluate the quality of urban settings and to improve their soundscape design (Aletta and Kang, 2015; Alves et al., 2015; Lionello et al., 2020; van Kempen et al., 2014; Yang and Kang, 2005). But due to its labor intensity, this approach is only feasible for a limited amount of urban settings. In the field of public health, soundscapes are also used to study associations between the AE, human health and well-being (Aletta et al., 2018) adding to the very well developed field of noise pollution (Babisch et al., 2005; Orban et al., 2016; Peris et al., 2019; WHO, 2018). However, while the impact of noise in urban regions has been studied for a long time, less is known about the (urban) AE as a composite of several sources separate from noise (Kang et al., 2016).

Although research on the urban AE gained traction in recent years, sophisticated methods to quantify its complex properties on a larger scale are still scarce. This is especially true for big audio datasets, which are so extensive that listening to the files becomes no longer feasible. To date, few approaches have been used to quantify large datasets of the urban AE. Classical approaches reach their limits when it comes to analyzing longer recording periods (e.g. several months) (Gage et al., 2017). In recent years, sound event classification using machine learning approaches became more popular (Phillips et al., 2018; Sethi et al., 2022; Stowell et al., 2019; Ulloa et al., 2018), but is still not ready to be deployed unconfined (Alcocer et al., 2022). In psychoacoustics, mostly smaller field studies have been conducted (Hall et al., 2013; Ma et al., 2021; Montoya-Belmonte and Navarro, 2020; Raimbault et al., 2003), and the research focus is on the relationship between acute human perception and psychoacoustic indices in the urban environment. Therefore, psychoacoustic indices of the AE have not yet been extensively studied in high temporal or spatial resolution over longer periods. In contrast, audio recordings in ecoacoustics are often carried out at different sites over a longer period (Farina, 2013; Pijanowski et al., 2011). However, as ecoacoustics aims to investigate environmental sound to derive, e.g. biodiversity, its methods were developed for the implementation in natural areas. Thus, the application in urban areas is difficult, as characteristic frequency patterns of biophonic sound sources (e.g. birds) often overlap with patterns from antropophonic sound sources (e.g. cars) (Bradfer-Lawrence et al., 2019; Fairbrass et al., 2017; Haselhoff et al., 2022b). In addition, just recently Alcocer et al. (2022) showed in a meta-analysis of research from the last decade that the most commonly used ecoacoustic indices were only moderately related to biodiversity – while being applied in natural areas. They conclude that further research on ecoaocustic indices as well as the development and application of more effective methods is needed. This call aligns with a general call for more sophisticated methods to analyze extensive (urban) audio data (Fairbrass et al., 2017; Gage et al., 2017; Jiang et al., 2022; Towsey et al., 2014).

We take this as an opportunity to elaborate complex networks (CN) for the field of urban AE analyses. Over the last decades, CNs became a powerful tool in the characterization of complex real-world systems as they inherently account for the high dimensionality and complex topology of the observed interactions. For instance, they were successfully applied to model social networks, the World Wide Web, climate dynamics and brain activities (Achard et al., 2006; Albert et al., 1999; Barabási, 2013; Bullmore and Sporns, 2009; Donges et al., 2009; Newman, 2018; Stam and Reijneveld, 2007). Especially the latter is similar to the way we approach CNs for the urban AE. Here – in contrast to structural networks, which are based on physical connections – functional networks are constructed from statistical dependencies, "regardless of whether the nodes are physically connected" (Boashash et al., 2016). It is shown that complex networks represent an effective framework to characterize scale-specific correlations, which is of high relevance for a broad range of nonlinear real-world systems (Agarwal et al., 2019; De Domenico, 2017). Overall, complex networks have only rarely been used to analyze audio recordings, e.g. for clustering music based on melodic lines (Ferretti, 2017; Gomez et al., 2014). To the best of the knowledge of the authors, no applications based on the time-frequency domain are yet available – especially in regards to the urban environment.

In this work, we (i) describe all necessary steps of how CNs can be constructed from large-scale acoustic data and (ii) evaluate this process on approx. 1 million minutes of audio recordings from 23 different sites in Bochum, Germany. Here, the foundation for constructing complex networks for the urban AE build upon the concept that high correlations between frequency bins indicate the presence of particular sound sources (Nichols and Bradley, 2019). Therefore, statistical interrelationships resemble the overall composition of the AE and can be used to distinguish between different urban settings (Haselhoff et al., 2022a). As a network measure, the average shortest path length (ASPL) is used, which measures the number of connections and the topology of these connections in a network. We will focus on the ASPL diel cycle of each site, as previous research showed good results to characterize AEs through their hourly variations (Bradfer-Lawrence et al., 2019; Fuller et al., 2015; Lawrence et al., 2022; Pieretti et al., 2015). To identify groups of similar diel cycles, hierarchical cluster analysis is used. The clusters are then evaluated by using the land use mix (LUM) around each site as reasonable proxy for the AE, as the urban environment has a huge impact on the AE (Kang and Schulte-Fortkamp, 2016). Our goal is to introduce CNs as a tool for analyzing the complex structure of the urban AE and, thus, to enable the application of the vast variety of methods already developed in the research field of complex networks.

2 Data

2.1 Audio Data

For our work, we use data from the SALVE study. Briefly, 50 3-min audio files have been recorded daily at 84 locations in Bochum since 2019. Meanwhile, data is available over a period of more than three years. Here, we use a subset from 23 different locations from May 2019 to the end of February 2020 (defined in Haselhoff et al. (2022c) as AAP_{24}). The choice of the endpoint is motivated by excluding the changes to the AE caused by the corona pandemic (Hornberg et al., 2021). Recordings were made using *Wildlife Acoustics SM4 recorders* with

a SMMA2 microphone (Wildlife Acoustics, 2020). The devices were mounted at a height of approx. 1.65 m (DIN ISO 12913-1:2018-02) and programmed to record 3-minute recordings every 26 minutes at a sampling frequency of 44.1 kHz and 16 bit depth.

To retrieve information about the frequency spectrum, we calculate a Fast Fourier Transform for all recordings of our dataset, sort the values into 1024 equally sized bins (from 0 to 22,050 Hz; bin width=21.5 Hz; no spectral weighting) and average the values energetically inside each bin (Haselhoff et al., 2022a). As the magnitude of variability broadly differs between low and high frequencies, we align them by a log-transformation. Following previous research, we focus on the frequency range from 0 to 13 kHz, as frequencies above 13 kHz are only rarely occupied in the urban AE (Bradfer-Lawrence et al., 2019; Haselhoff et al., 2022a).

2.2   Land use types

For the initial definition of the land use type (LUT) for all 23 sites, the original LUT (defined by the Regional Association for the Ruhr Area (2020)), photographs and assessments of the respective recording sites were considered and later discussed between all team members. For a more comprehensive overview of the built environment around the devices, we calculated the land use mix (LUM) for all devices in a radius of 50 m around all recording locations, using the land use definition of the Regional Association. To describe the LUM, we selected the ten largest LUTs (which in total occupy more than 94% of the buffer area) to prevent the inclusion of very small and uncommon LUTs (Fig. A1).

In summary, we analyzed a dataset that consists of 319,385 3-min recordings made at 23 different locations, from 7th May 2019 to 25th of February 2020. In total, this equals 958,155 minutes or 665 days of consecutive audio recordings.

3   Methods

3.1   Pre-Processing

Pre-Processing consisted of two steps: (i) the plausibility check of the data and (ii) De-Noising.

3.1.1   Plausibility Check

A detailed description of the plausibility check for SALVE can be found in Haselhoff et al. (2022c). In summary, faulty recordings or recordings with device induced sounds (e.g. rattling) were removed. Additionally, a number of ecoacoustic indices (NDSI, BIO, ADI, AEI, ACI, Hf, Ht, H, M, NP) (Sueur, 2018) as well as sound pressure indices (LAmin, LAmax, LAeq) were calculated for all recordings. Following, all indices were examined for anomalies by means of descriptive statistics to exclude erroneous recordings.

3.1.2   De-Noising

To improve the robustness of our analyses, we use Principal Component Analysis (PCA) to remove uncorrelated noise for each frequency bin (Abdi and Williams, 2010; Shannon, 1948). Here, we separate the temporal variability of each frequency bin into components, representing linear combinations of the original

data. Ordered by their eigenvalues, we extract the leading components for each frequency bin per location, which describe ≥ 95 % of the variance. We obtain the de-noised frequency bin time series by reconstructing each signal only from these leading components (i.e. we perform the inverse transformation).

3.2   Complex networks

Complex networks – in their simplest form – can be described as a collection of joined nodes (Newman, 2018). They can be represented by a binary adjacency matrix (for unweighted networks and networks without multi- and self-edges) that defines which nodes are connected in the network. Following this concept, we construct the adjacency matrices by defining the frequency bins as the nodes and the presence of a connection between two nodes dependent on the strength of the correlation between two frequency bins.

3.2.1   Constructing acoustic environment networks

We use complex networks and selected network quantifiers to investigate the spatial coherence of different AEs. Frequency correlation matrices (FCMs) are used as the basis for the adjacency matrix, as we want to capture the strongest correlations between frequency bins. As the dimension of FCMs is only dependent on the number of frequency bins chosen and FCMs are always symmetrical, the construction of CNs is straightforward. The first step to create a complex network from acoustics data is to calculate the FCM. Considering the diel cycle, we calculate correlations between all frequency bins for each device, grouped by daytime (i.e. 24 hours), resulting in 24 FCMs per device. The coefficient of determination (R^2) is used to measure the proportion of explained variance between two frequency bins. R^2 quantifies the strength of the relationship between frequency bins and ranges from 0 to 1. However, as we are only interested in the strongest similarities (between frequency bins), we apply a threshold to derive the adjacency matrix from the FCM (i.e. setting all R^2 values above the threshold to one , i.e. frequency bins are connected; and all values below to zero, i.e. frequency bins are not connected). To illustrate the process, Figure 2 shows two examples for the LUTs "Main Street" and "Urban Forest", depicting every step from the FCM, to thresholding, to the adjacency matrix and its respective network representation.

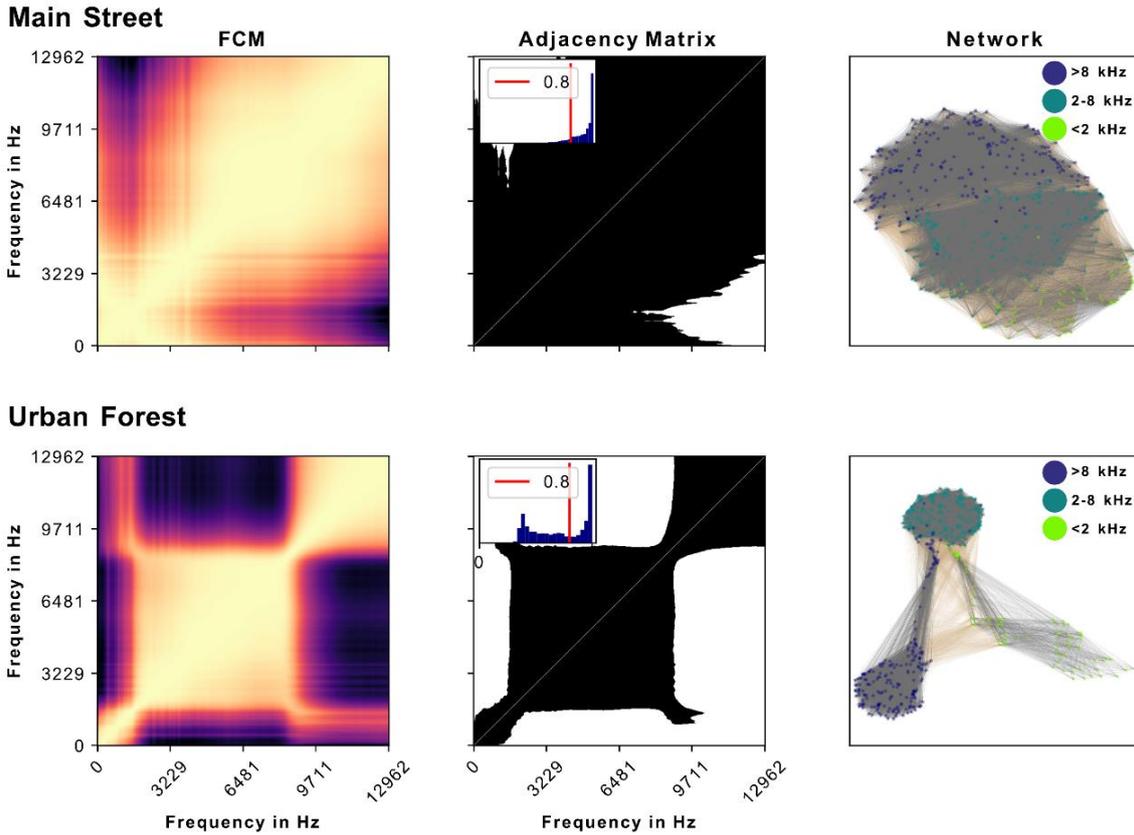**Main Street**

Urban Forest

Figure 1: Illustration of the procedure to build a simple graph from frequency correlation matrices (FCM) for two examples ("Main Street" and "Urban Forest"). The colors of the FCM represent the R^2 value from 0 (dark) to 1 (bright). The inset in the adjacency matrix depicts the distribution of R^2 values of the FCM and shows an arbitrarily chosen threshold (0.8) to create the binary adjacency matrix. The node colors for the networks were chosen accordingly to the definition of antropophonic (<2 kHz) and biophonic (2-8 kHz) sounds. From this example, it can already be seen that frequency bins in natural areas tend to build more differentiated clusters and that they are closer to the initial definition of antropophonic and biophonic frequency ranges than the frequency bins in heavily trafficked areas.

3.2.2   Defining the threshold

A threshold can either be set by constraining correlations by an arbitrary lower threshold value – e.g. by saying that we are only interested in frequency bins that correlate with $R^2 > 0.8$ or higher (Fig. 1) – or by a more informed data-adaptive choice. In our work, we use the latter approach by deriving the threshold from the individual data of each site. For this, we consider the probability distribution of R^2 values, which allows the identification of multimodality (Toubiana and Maruenda, 2021). Multimodal distributions indicate a mixture of multiple underlying distributions from different groups. We use Kernel Density Estimation (Scott and Sheather, 1985) to sample from the R^2 distribution ($k(R^2)$) and use peak-, low-point detection to identify the group with the highest R^2 values. This group represents the frequencies with the strongest connections, indicating groups of sound sources that co-evolve similarly on a daily-time scale. If no multimodal distribution can be identified, we define the threshold by dividing the peak value of $k(R^2)$ by Euler's number: $peak\left(k(R^2)\right)/e$, as all R^2 distributions we analyzed exhibit an exponential increase close to $R^2 = 1$. Then, we choose the highest x-axis intercept where the kernel density distribution crosses $peak\left(R^2\right)/e$ on the y-axis to define the threshold for this distribution. This way, we still identify the group with the strongest connections.

Pseudo-Code for threshold identification as well as two examples can be found in Figure 2. In this work, we calculate the threshold for all 24 FCMs of one site and take the median of all 24 values as the threshold for the specific location. This ensures comparability between daytimes and improves the robustness against rare outliers.

```
Input: FCM Matrix
KernelDensity = EstimateKernelDensity(FCM)
Sample = sample(n=100, with equal steps from 0 to 1, from KernelDensity)
Peaks = FindPeaks(Sample)
Lows = FindLows(Sample)
if number of Lows > 0 AND number of Peaks > 1:              #multimodal case (a)
        Threshold = Maximum value of Lows
else:                                                       #unimodal case (b)
        X = Sample[Maximum value of Peaks]/e
        Threshold = x-axis intercept where the maximum value of Sample == X
Output: Threshold
```
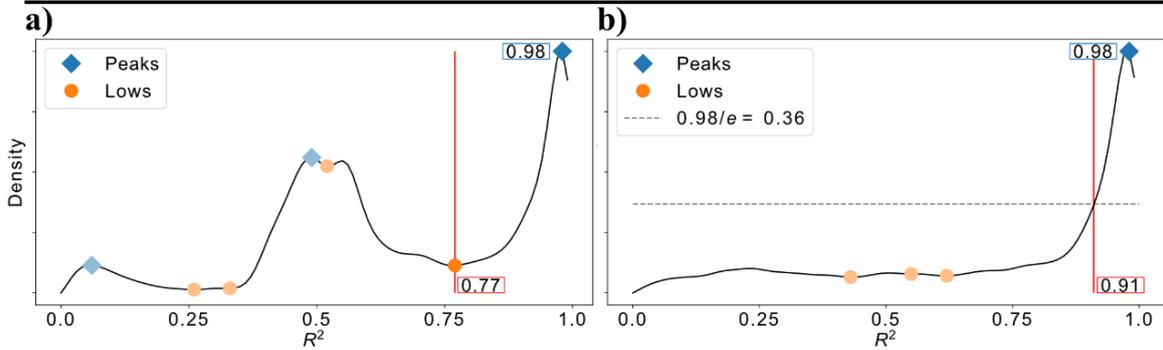

Figure 2: Pseudo-Code for choosing the threshold of a frequency correlation matrix. Below, two examples are depicted: (a) for a multimodal distribution and (b) for a unimodal distribution of R² values.

3.2.3   Complex network measures

After the network is constructed, a plethora of quantitative network measures become available (Newman, 2018). We investigate the utility of the network's Average Shortest Path length (ASPL) for the studied networks. ASPL can be defined as (Barabási, 2013):

$$ASPL = \sum_{\substack{s,t\in V \\ s\neq t}} \frac{d(s,t)}{n(n-1)}$$

Where V is the set of nodes in the network, d is the shortest path between respective nodes s and t, and n is the number of nodes in the network. Thus, ASPL can be described as the minimum number of "steps" it takes to "go" from each node to all other nodes, normalized by the total number of nodes in the network. Therefore, its value is dependent on the number of connections and the topology of these connections. For example, we can see that the nodes for "Main Street" in Figure 1 are (i) more frequently connected and that (ii) their connections are more homogeneously distributed than in "Urban Forest". In the latter, we can see clear rectangular structures, which makes it more "complicated" to get from one node of one rectangle to nodes of another rectangle. Accordingly, the ASPL for "Main Street" is lower (1.12) than for "Urban Forest" (1.66). In our case, low ASPL suggests that frequency bins are highly correlated with each other and fewer bins build distinct communities. Thus, ASPL for the urban AE can be interpreted as an "acoustic dominance" index for the time-

frequency spectrum. If single sound sources (like traffic) are the reason for many high frequency correlations throughout the whole spectrum ('high dominance'), then ASPL will be lower. If multiple sound sources form distinct correlation communities ('low dominance'), ASPL will be higher. In our work, we calculate ASPL for all networks of the diel cycle for each recording site, resulting in 23 time series over 24 hours (Fig. 3).

3.3   Clustering

To determine which of the site-specific AEs exhibit similar diel cycles of "acoustic dominance", we cluster the devices based on their ASPL variations over the day. For this, we smooth the diel cycle by calculating the ASPL for each hour as the average between its value and the values of the hour before and after. This way, we try to mitigate transition effects, as recordings earlier/later in an hour will be more similar to recordings before/after that hour. Subsequently, we calculate the Pearson correlation between the ASPL variations for all recording sites. Next, we use hierarchical clustering, using complete-linkage (Brian S. Everitt, 2011) to group devices with similar diel cycles.

4   Results

4.1   Diel cycle of average shortest path length

The overall mean ASPL for each site/automatic aural device (AAD) ranges from 1.59 (AAD6; Residential Street) to 3.85 (AAD2; Small Garden near House) (Fig. 3). It can be observed that more built-up areas tend to have a lower mean ASPL than more natural areas (Fig. A1). However, this pattern does not hold true for all locations. For example, AAD23 (Commercial Area) shows one of the highest ASPL values (2.76) though the LUM is predominantly defined by commercial area. Additionally, AAD17 (Urban Agricultural Land) and AAD14 (Main Street) have similar mean ASPL values (~2.1) even though AAD17 is surrounded by mainly forest area and AAD14 by road area (Fig. A1). As our research approach is tailored towards the analysis of diel cycles, it was to be expected that the absolute values of the data may not provide a clear distinction between the LUMs of all locations being studied.

In contrast, the examination of the diel cycles from the 23 sites reveals numerous comprehensible patterns that validate the utility of the proposed method (Fig. 3). ASPL values above average in the beginning of the day are almost exclusively found in more built-up areas (referring here to commercial area, main street and residential street). In addition, these are the only LUTs where multiple AADs have below average ASPL values between 7 h and 20 h (AAD6, 7, 10, 13 and 23). Furthermore, AAD11, 14 and 15 exhibit a unique pattern, with below average ASPL values between 0 h and 8 h, followed by a constant above average value for the rest of the day. However, all LUTs except commercial areas, main streets, and residential streets follow a similar course: At 0 h, ASPL starts below average, with the lowest values at around 2 h to 3 h. Following, ASPL increases and reaches above mean values at around 5 h to 6 h with peaks at around 8 h, after which the ASPL decreases and the sites behave more heterogeneously but in three characteristic patterns. There is either (i) a decrease of ASPL for the rest of the day (AAD4, 8 and 16), (ii) an increase until around 16 h to 17 h (AAD3, 5, 12 and 21) or (iii) a decrease, followed by an increase with a peak at around 20 h (AAD17, 18, 19, 20 and 24). The only

exception to this pattern is AAD1 where we find a diel cycle more similar to that of AAD7 ("Main Street") and AAD10 (residential street). The reason for this is most certainly the closeness to the highway (Fig. A1), which is located directly behind the garden. Another distinctive feature is that areas in proximity to streets show lower ASPL variance between daytimes (Fig. B1). While those areas rarely deviate by more than 0.1, all other LUTs often deviate by an ASPL value of up to 0.5 (AAD21) from the mean. This suggests a more monotonous urban AE throughout the day for roadside areas in contrast to all other LUTs.
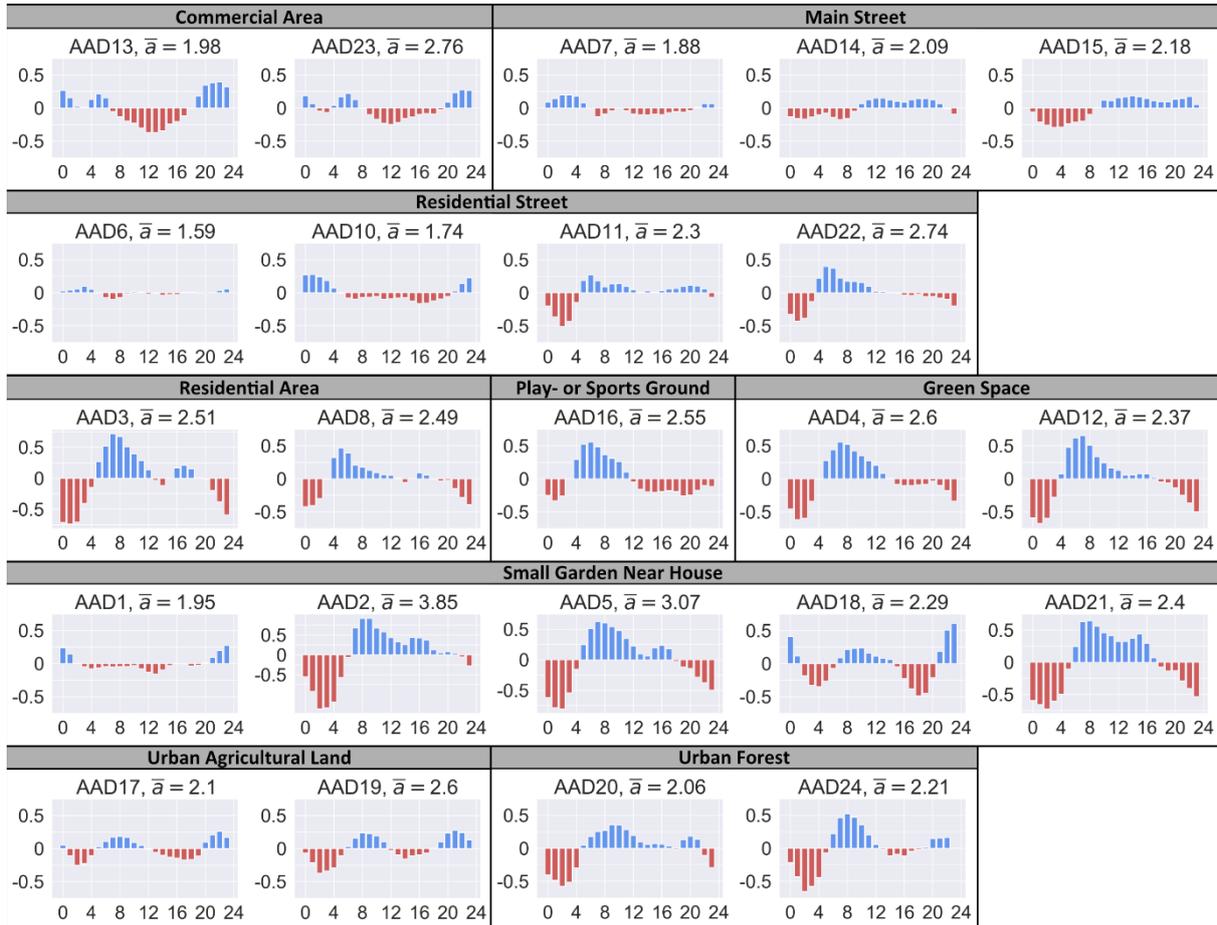

Figure 3: Average Shortest path length (ASPL) by daytime, grouped by land use type. Depicted are all 23 recording sites (Automatic Aural Devices (AAD)) and their respective ASPL diel cycle. ASPL values are centered on the mean to put emphasis on the individual course of ASPL. Blue color means that the value for the respective hour is above and red color that the value is below the mean. The mean of all ASPL values per site is given by $\bar{a}$.

4.2   Cluster analysis of ASPL diel cycles

We carry out a cluster analysis to reveal groups of LUTs that exhibit similar diel variations of ASPL (see 3.3). Hierarchical clustering of site-specific ASPL diel cycles gives rise to four to seven distinct clusters (Fig. 4). While there are several techniques to determine the exact number of clusters in hierarchical clustering (e.g. dynamic tree cutting (Langfelder et al., 2008) or elbow method) the most adequate technique depends on the studied data and research question (Brian S. Everitt, 2011). Based on the well-organized group structures in Figure 4, we heuristically define six clusters (color-coded from light yellow to black in Fig. 4). However, it should be noted that the exact number of clusters does not change their interpretation. In the following, the reason for this as well as the commonalities and differences in LUMs for all sites are presented.

Cluster I (AAD6, 7 and 10) can be labelled as "roadway dominant land cover'". The LUM of all three locations are more than 20% road areas and located in the proximity of residential areas (Fig. A1). These are the devices whose ASPL value starts above and declines below its average value throughout the diel cycle. Looking at photographs of the sites (Fig. 5) and considering on-site visits, this pattern most likely reflects the traffic volume, whose course over the day is inversely related to the ASPL value (Straßenwesen, 2022). Cluster II behaves relatively similar to the first one as these are the three additional devices where the ASPL cycle starts below average (AAD1, 13 and 23). This is reflected in Figure 4, with most of them correlating moderately with the AADs from Cluster I and forming the first distinct square. It stands out that AAD1 is located in a garden, but its similarities to the other AADs of the cluster is explained by its adjacency to a highway. In the photo (Fig. 5) the soundproof wall can be seen. The same applies to AAD23, where the highway is just located at the end of the street on the photograph. Considering this, Cluster II can be described as highly influenced by highway traffic and commercial transport.

In contrast, clusters III and IV are represented by sites whose diel cycles are much more divergent than those of clusters I and II. Accordingly, the LUM around those recording stations is composed quite differently. Cluster III includes AAD2, 21, 24, 11 and 20. Their LUMs are dominated by gardens (ø =17%) and forest area (ø =25%) and very little road area (ø=7%) (Fig. A2). Thus, cluster III could be described as forests or gardens distant from road noise. The only exception to this LUT description in cluster III is AAD11 (residential street). However, upon further inspection we find it is located on a traffic-calmed tree-lined street adjacent to an urban forest patch, thereby fitting in well with the description of forest or garden even though it sits within a residential matrix. Overall, the cluster's ASPL variation is defined by the highest values at around 8 h, followed by a decrease and then a second smaller peak at around 20 h, probably reflecting bird chorus. The exception is AAD21, which exhibits the second peak around 16 h and is also very similar to the sites included in Cluster IV. Comparing the cycles between the AADs from Cluster III and IV, it becomes obvious that most of them correlate moderately to highly. This can also be seen from the clearly recognizable quadrilateral structure these devices build, forming the most prominent distinct structure in Figure 4. Accordingly, Cluster IV represents the biggest cluster, including seven sites (AAD16, 4, 3, 5, 8, 12 and 22). Considering the photographs as well as the LUMs, we see that these sites are predominantly defined by public and private green space within a residential matrix in proximity to tree-lined traffic-calmed streets. The diel cycles resemble those from Cluster III, but in most cases, Cluster IV is missing the second peak in the afternoon hours and the ASPL value falls below average after approx. 16 h.

Cluster V includes AAD14 and 15. This cluster exhibits distinct diel cycles and does not resemble other AADs. This is underscored by the LUMs of the included sites (Fig. A2). Both recording devices are located next to a highly trafficked main street with streetcar transport. The ASPL cycle starts around the same value below average, until around 8 h, when it increases slightly above average, while remaining relatively constant, indicating little variation of the AE after 8 h. Cluster VI includes sites AAD18, 17 and 19 with a LUM dominated by large agricultural areas within the overall urban matrix but generally far from roads. Although AAD18 is located in a garden, an agricultural field is located right behind the gate depicted on the photograph. Accordingly, their diel cycles are distinct, with night and morning phases from 0 h to 12 h similar to the

forested Cluster III, followed by an afternoon phase similar to Cluster I until about 20 h, after which the pattern returns to match cluster III.

Summarizing, distinct clusters are identified, exhibiting high intra- and low inter-correlations between diel ASPL profiles. The few exceptions are AAD17 and 19 from urban agricultural land, which also correlate highly with sites from Cluster III, namely AAD20 and 24 from Urban Forests and AAD11 from a residential street.
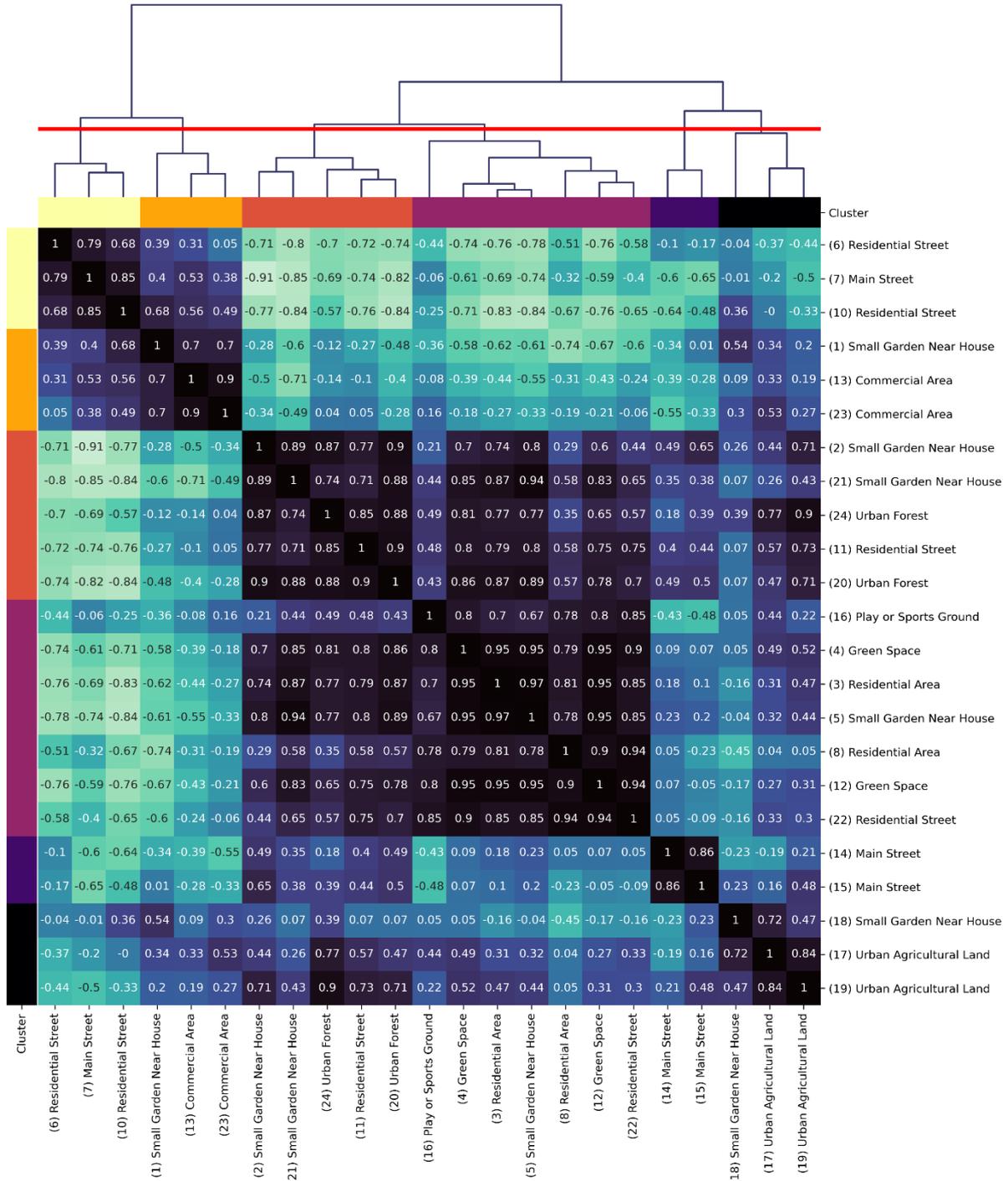

Figure 4: Hierarchical clustering of correlations between the ASPL diel cycles of all recording sites. The values inside the squares show the Pearson correlation coefficients between the respective sites. The color of the squares corresponds to the strength of the correlation (-1 to 1). The red line in the dendrogram represents the cut-off value to determine the clusters.

Figure 5: Photographs of all sites, ordered into their respective cluster. The color coding as well as the order of the AADs corresponds to those depicted in Figure 4. More details regarding the LUM for each cluster can be found in Figure A2.

5 Discussion

The goal of this work was to introduce complex networks as a tool to analyze the urban AE and to demonstrate its application with one of most comprehensive datasets of the urban AE, comprising roughly one million minutes of audio recordings. Our results show that mean ASPL values over the day tend to be higher in forested green spaces and residential areas, gardens, and agricultural areas than in commercial areas, main streets, and residential streets. This is a promising indication that the mean ASPL value can differentiate between different urban AEs. However, this does not always hold true, as one of the highest ASPL values occurs in a commercial area (AAD23) surrounded only by roads and residential areas. On the other hand, AAD23 has large street trees and the highway at the edge of the LUM buffer includes a low noise wall and noise reducing pavement (Fig. 5). This could be the reason that the ASPL is more in line with AADs in clusters III and IV, but this conclusion needs further investigation. At this point, the high ASPL value at AAD23 simply means that the "acoustic dominance" is similar to those in Clusters III and IV. Therefore, we find that the AE cannot be derived directly from the mean ASPL values.

However, analyzing the ASPL diel cycle produced consistent results. We observed a similar ASPL course over the day for sites with similar LUMs. We found six clusters exhibiting distinct ASPL trends over 24 h. Most of them form clusters for which it is reasonable, based on their LUMs, to have a similar AE. Cluster I and II are more similar to each other than to any other cluster and both can be assumed to be highly influenced by traffic. While cluster I comprises readily frequented roads in proximity to residential areas, sites from cluster II are additionally in proximity to commercial areas and highways.

Two clusters form the largest distinct rectangular structure identified. One cluster encompasses areas with forested or heavily vegetated land cover (Cluster III), while the other consists of traffic-calmed areas with mature street trees (Cluster IV). Both clusters are similar, as reflected by similar diel cycles of ASPL, although Cluster III has above average values after around 16 h and Cluster IV tends to become below average at that time. These findings suggest that Cluster III and IV share certain characteristics of the AE. One less intuitive assignment is that of AAD11 to Cluster III, which appears to fit better with Cluster IV in terms of its LUM characteristics (i.e. it is located close to a road and has much less vegetated cover than other sites in Cluster III). One possible explanation for this is that the surrounding areas designated as "community demand areas" and "public and private green areas" have dense tree cover, which could significantly influence the AE through biophonic sounds. A sample examination of AAD11 did indeed reveal that prominent bird sounds regularly occur in this area, but the exact reason remains subject to further research. In contrast, Cluster V is again formed by very similar sites (AAD14 and 15), both located in close proximity to main roads with streetcars. This shows that CNs of the urban AE, measured with ASPL, are able to identify sites with LUMs dominated by a specific land use. The same applies to Cluster VI, which is characterized by its agricultural and forested areas as well the absence of built-up areas. Furthermore, unlike most clusters, sites in Cluster VI also correlate moderately to highly with sites in Cluster III, especially those located in urban forests (AAD20 and 24). It can be assumed that these matches are also due to the high percentage of forest vegetation and the low percentage of built-up area around those sites.

In summary, complex networks based upon FCMs generate promising results in distinguishing urban sites with similar LUMs. The clusters are characterized by high intra- as well as low inter-correlations of the ASPL diel cycle. In particular, strongly distinct sites with very high traffic impact (Cluster I and V) as well as forested areas, gardens, and residential areas with traffic calming and street trees (Clusters III and IV) are consistently recognized. Additionally, sites that would be mismatched based on their initial land use type (AAD1 and 18) show strong resemblance to the other sites inside their clusters, e.g. being located directly to the edge of a highway or agricultural land respectively. These results highlight the capabilities of functional complex networks to represent the statistical interrelationships between frequency bins over time. Correlations between frequency bins provide valuable information about related sound sources, and thus, they reflect distinct behavior of AEs present. However, as these correlations do not always occur between the same frequency bins or the same number of frequency bins, a multitude of community structures arise. With our application of complex networks, the topology of the formed frequency communities is captured. This underlines the potential of using complex networks and its corresponding metrics to gain insights into the complex interdependencies and patterns that emerge in AEs. Considering that we only used one index (ASPL) to measure the CNs created in this work, it shows that complex networks hold a lot of potential to contribute to future analyses of the urban AE. It would be conceivable, that further indices are used (e.g. Modularity, Network Diameter or Degree Centrality (Barabási, 2013; Newman, 2018)). Furthermore, findings from the analysis of observational complex networks can inform novel approaches for model representations (e.g. stochastic block models (Faskowitz et al., 2018)). A special feature of this work is that we have concentrated on diel cycles, but concerning the possibility that FCMs can be formed for any recording groups, other time scales also become feasible. For instance, networks for days, weeks or months can be build or we could even analyze networks within single recordings. Finally, evolving networks could reveal transitions in the dynamics of the urban AE (Belykh et al., 2014).

Nevertheless, several limitations of this study need to be stressed. Regarding the definition of the correlation value threshold, we presented a method to determine the group with the highest R^2 for each individual urban site. The feasibility of defining constant thresholds for all sites, especially when it comes to analyzing a higher number of FCM (e.g. numerous days individually), needs to be evaluated in future research. In addition, it might be of interest to look at groups with moderate or lower R^2 values, which we found to be especially prevalent in sites with forested land cover. Another limitation of our work is that we only used ASPL as a measure for the CNs of the urban AE, but this measure requires fully connected networks (i.e. each node can be reached from all other nodes). In preliminary analyses for smaller time scales, this was found to not always be the case and thus, alternative measures (e.g. link density) might be more appropriate. Another limitation is that our analysis is only based on 23 urban sites in Bochum. The number of clusters based upon ASPL diel cycles might differ for other locations around the world and its performance needs to be evaluated for differing environments. Although the environment has a substantial influence on the AE, it can only be used as a proxy for the actual sound sources that are present at each site. Further research is needed to understand the precise role that biophonic and anthrophonic sounds play in shaping the ASPL diel cycles of these areas. As it is not feasible to listen to the recordings to identify specific sound sources, we cannot currently determine

their direct associations to specific ASPL values. To accomplish this, more sophisticated and robust methods need to be established, identifying the exact sound source composition of the urban AE.

6 Conclusion

In this work, we showed how to construct complex networks based on FCMs and emphasized the importance of defining the correlation threshold. We used ASPL as quantification of the networks properties, measuring the number of connections (i.e. number of highly correlated frequency bands) and the topology of those connections (i.e. if highly correlated frequency bins form distinct communities), creating a metric of so-called "acoustic dominance". Although the exact mechanisms of how specific sound sources shape the urban AE remain unsolved, we found substantial similarities in the diel cycle as well as LUMs between sites of similar LUM. Since this study is the first of its kind and substantial contributions to the description of the acoustic environment are already evident here, future analyses using complex networks should open up an interesting new branch of research. Thus, the application of a whole methodology based on CNs, which has already led to exceptional findings in many other fields, is enabled. The possibility to analyze data comprising hundreds of hours of acoustic recordings could make it a feasible tool to consider for research on the (urban) AE, complementing existing methods such as those of eco- and psychoacoustics.

Appendix A

Figure A1: Land use mix for all AADs. Depicted is the percentage of land use type area in a 50m radius buffer around each recording station. Depicted are the ten largest land use types, which in total occupy more than 94% of the 50m buffer area.
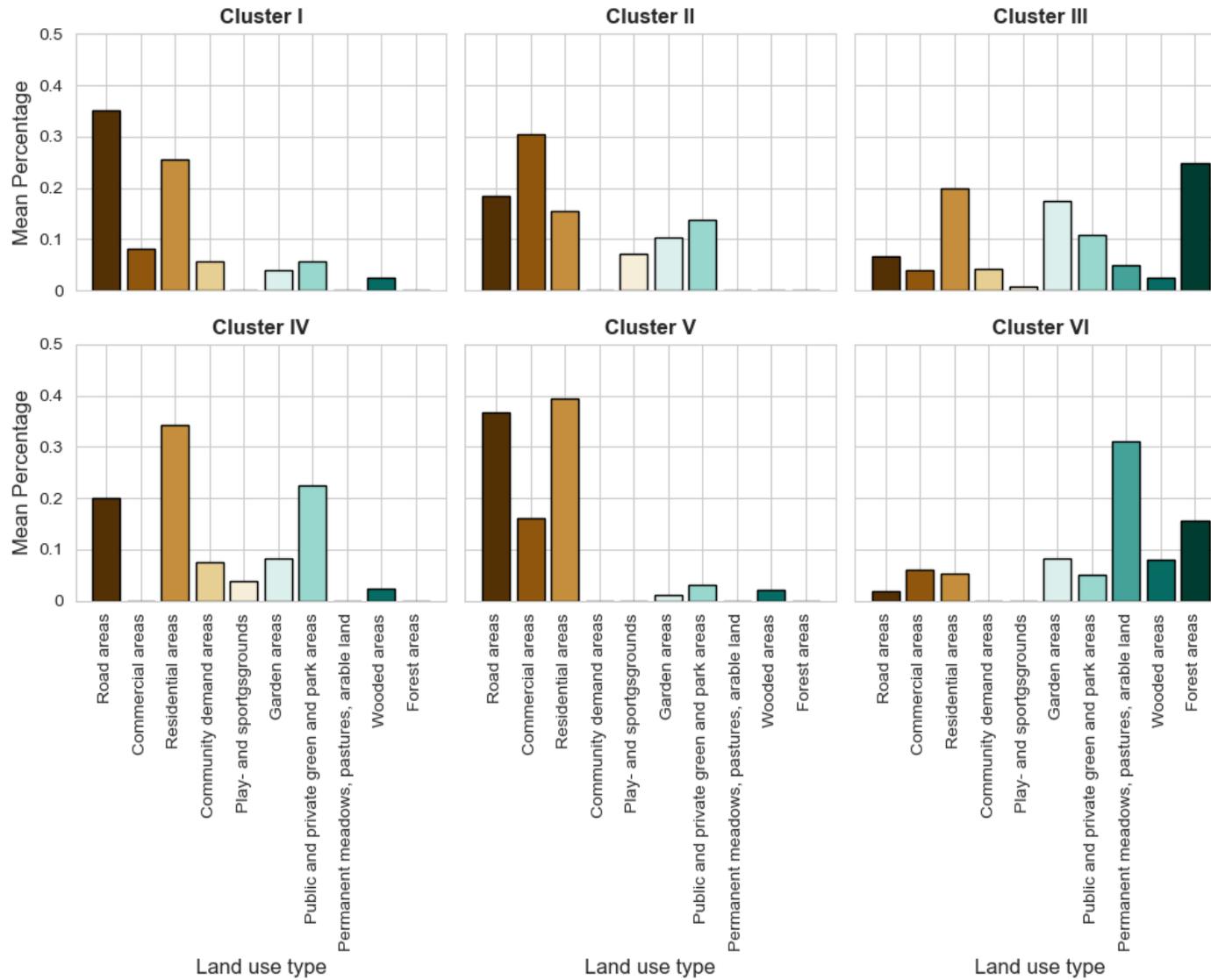
Figure A2: Average land use mix for all clusters. Depicted is the percentage of land use type area in a 50m radius buffer around each recording station, averaged by cluster. Depicted are the ten largest land use types, which in total occupy more than 94% of the 50m buffer area.

Appendix B

AAD_ID	Land Use Type	R^2-Threshold	ASPL	STD
1	Small Garden Near House	0.69	1.95	0.12
2	Small Garden Near House	0.76	3.85	0.72
3	Residential Area	0.75	2.51	0.46
4	Green Space	0.74	2.60	0.35
5	Small Garden Near House	0.75	3.07	0.46
6	Residential Street	0.72	1.59	0.06
7	Main Street	0.78	1.88	0.12
8	Residential Area	0.76	2.49	0.27
10	Residential Street	0.90	1.74	0.15
11	Residential Street	0.72	2.30	0.23
12	Green Space	0.67	2.37	0.40
13	Commercial Area	0.75	1.98	0.27
14	Main Street	0.91	2.09	0.13
15	Main Street	0.75	2.18	0.19
16	Play Or Sports Ground	0.74	2.55	0.30
17	Urban Agricultural Land	0.76	2.10	0.17
18	Small Garden Near House	0.72	2.29	0.34
19	Urban Agricultural Land	0.72	2.60	0.21
20	Urban Forest	0.77	2.06	0.31
21	Small Garden Near House	0.61	2.40	0.48
22	Residential Street	0.79	2.74	0.23
23	Commercial Area	0.75	2.76	0.18
24	Urban Forest	0.71	2.21	0.34

Table B1: Depicted are AAD_ID, the land use type of all sites, R^2-Thresholds (calculated as median from thresholds for all 24 hours of day), average shortest path length (ASPL; averaged over all ASPL values for 24 hours of day by device) and standard deviation (STD; calculated between all ASPL values for 24 hours of day).

7 References

Abdi, H., Williams, L.J., 2010. Principal component analysis. Wiley interdisciplinary reviews: computational statistics 2, 433-459.

Achard, S., Salvador, R., Whitcher, B., Suckling, J., Bullmore, E., 2006. A Resilient, Low-Frequency, Small-World Human Brain Functional Network with Highly Connected Association Cortical Hubs. The Journal of Neuroscience 26, 63.

Agarwal, A., Caesar, L., Marwan, N., Maheswaran, R., Merz, B., Kurths, J., 2019. Network-based identification and characterization of teleconnections on different scales. Scientific Reports 9, 8808.

Albert, R., Jeong, H., Barabási, A.-L., 1999. Diameter of the World-Wide Web. Nature 401, 130-131.

Alcocer, I., Lima, H., Sugai, L.S.M., Llusia, D., 2022. Acoustic indices as proxies for biodiversity: a meta-analysis. Biological Reviews 97, 2209-2236.

Aletta, F., Kang, J., 2015. Soundscape approach integrating noise mapping techniques: A case study in Brighton, UK. Noise Mapping 2.

Aletta, F., Oberman, T., Kang, J.J.I.j.o.e.r., health, p., 2018. Associations between positive health-related effects and soundscapes perceptual constructs: A systematic review. Int. J. Environ. Res. Public Health 15, 2392.

Alves, S., Estévez-Mauriz, L., Aletta, F., Echevarria-Sanchez, G.M., Romero, V.P., 2015. Towards the integration of urban sound planning in urban development processes: The study of four test sites within the SONORUS project. Noise mapping 2.

Babisch, W., Beule, B., Schust, M., Kersten, N., Ising, H., 2005. Traffic noise and risk of myocardial infarction. Epidemiology 16, 33-40.

Barabási, A.-L., 2013. Network science. Philosophical Transactions of the Royal Society A: Mathematical, Physical and Engineering Sciences 371, 20120375.

Belykh, I., di Bernardo, M., Kurths, J., Porfiri, M., 2014. Evolving dynamical networks. Physica D: Nonlinear Phenomena 267, 1-6.

Boashash, B., Stevenson, N., Rankine, L., Azemi, G., Sejdić, E., Aviyente, S., Akan, A., Mert, A., Dong, S., Omidvarnia, A., 2016. Time-frequency methodologies in neurosciences. Elsevier Inc.

Botteldooren, D., Andringa, T., Aspuru, I., Brown, L., Dubois, D., Guastavino, C., Lavandier, C., Nilsson, M., Preis, A., 2013. Soundscape for European cities and landscape: understanding and exchanging, COST TD0804 Final conference: Soundscape of European cities and landscapes. Soundscape-COST, pp. 36-43.

Bradfer-Lawrence, T., Gardner, N., Bunnefeld, L., Bunnefeld, N., Willis, S.G., Dent, D.H.J.M.i.E., Evolution, 2019. Guidelines for the use of acoustic indices in environmental research. Methods in Ecology and Evolution 10, 1796-1807.

Brian S. Everitt, S.L., Morven Leese, Daniel Stahl, 2011. Cluster Analysis, 5th Edition ed. John Wiley & Sons, Ltd, London, UK.

Bullmore, E., Sporns, O., 2009. Complex brain networks: graph theoretical analysis of structural and functional systems. Nature Reviews Neuroscience 10, 186-198.

De Coensel, B., Bockstael, A., Dekoninck, L., Botteldooren, D., Schulte-Fortkamp, B., Kang, J., Nilsson, M.E., 2010. The soundscape approach for early stage urban planning: a case study, INTER-NOISE and NOISE-CON Congress and Conference Proceedings. Institute of Noise Control Engineering, pp. 3294-3303.

De Domenico, M., 2017. Multilayer modeling and analysis of human brain networks. GigaScience 6, gix004.

DIN ISO 12913-1:2018-02, Acoustics - Soundscape - Part 1: Definition and conceptual framework (ISO 12913-1:2014).

Donges, J.F., Zou, Y., Marwan, N., Kurths, J., 2009. Complex networks in climate dynamics. The European Physical Journal Special Topics 174, 157-179.

Fairbrass, A.J., Rennert, P., Williams, C., Titheridge, H., Jones, K.E., 2017. Biases of acoustic indices measuring biodiversity in urban areas. Ecological Indicators 83, 169-177.

Farina, A., 2013. Soundscape ecology: principles, patterns, methods and applications. Springer, Dordrecht.

Faskowitz, J., Yan, X., Zuo, X.-N., Sporns, O., 2018. Weighted Stochastic Block Models of the Human Connectome across the Life Span. Scientific Reports 8, 12997.

Ferretti, S., 2017. On the modeling of musical solos as complex networks. Information Sciences 375, 271-295.

Fuller, S., Axel, A.C., Tucker, D., Gage, S.H., 2015. Connecting soundscape to landscape: Which acoustic index best describes landscape configuration? Ecological Indicators 58, 207-215.

Gage, S.H., Towsey, M., Kasten, E.P., 2017. Analytical Methods in Ecoacoustics, Ecoacoustics, pp. 273-296.

Gomez, F., Lorimer, T., Stoop, R., 2014. Complex Networks of Harmonic Structure in Classical Music, in: Mladenov, V.M., Ivanov, P.C. (Eds.), Nonlinear Dynamics of Electronic Systems. Springer International Publishing, Cham, pp. 262-269.

Hall, D.A., Irwin, A., Edmondson-Jones, M., Phillips, S., Poxon, J.E.W., 2013. An exploratory evaluation of perceptual, psychoacoustic and acoustical properties of urban soundscapes. Applied Acoustics 74, 248-254.

Haselhoff, T., Braun, T., Hornberg, J., Lawrence, B.T., Ahmed, S., Gruehn, D., Moebus, S., 2022a. Analysing Interlinked Frequency Dynamics of the Urban Acoustic Environment. International Journal of Environmental Research and Public Health 19, 15014.

Haselhoff, T., Hornberg, J., Fischer, J.L., Lawrence, B.T., Ahmed, S., Gruehn, D., Moebus, S., 2022b. The acoustic environment before and during the SARS-CoV-2 lockdown in a major German city as measured by ecoacoustic indices. The Journal of the Acoustical Society of America 152, 1192-1200.

Haselhoff, T., Lawrence, B., Hornberg, J., Ahmed, S., Sutcliffe, R., Gruehn, D., Moebus, S., 2022c. The acoustic quality and health in urban environments (SALVE) project: Study design, rationale and methodology. Applied Acoustics 188, 108538.

Hornberg, J., Haselhoff, T., Lawrence, B.T., Fischer, J.L., Ahmed, S., Gruehn, D., Moebus, S., 2021. Impact of the COVID-19 Lockdown Measures on Noise Levels in Urban Areas—A Pre/during Comparison of Long-Term Sound Pressure Measurements in the Ruhr Area, Germany. International Journal of Environmental Research and Public Health 18, 4653.

Jiang, L., Bristow, A., Kang, J., Aletta, F., Thomas, R., Notley, H., Thomas, A., Nellthorp, J., 2022. Ten questions concerning soundscape valuation. Building and Environment 219, 109231.

Kang, J., Aletta, F., Gjestland, T.T., Brown, L.A., Botteldooren, D., Schulte-Fortkamp, B., Lercher, P., van Kamp, I., Genuit, K., Fiebig, A., 2016. Ten questions on the soundscapes of the built environment. Building and Environment 108, 284-294.

Kang, J., Schulte-Fortkamp, B., 2016. Soundscape and the built environment. CRC press Boca Raton, FL, USA:.

Kasten, E.P., Gage, S.H., Fox, J., Joo, W., 2012. The remote environmental assessment laboratory's acoustic library: An archive for studying soundscape ecology. Ecological informatics 12, 50-67.

Krause, B., Farina, A., 2016. Using ecoacoustic methods to survey the impacts of climate change on biodiversity. Biological Conservation 195, 245-254.

Langfelder, P., Zhang, B., Horvath, S., 2008. Defining clusters from a hierarchical cluster tree: the Dynamic Tree Cut package for R. Bioinformatics 24, 719-720.

Lawrence, B.T., Hornberg, J., Haselhoff, T., Sutcliffe, R., Ahmed, S., Moebus, S., Gruehn, D., 2022. A widened array of metrics (WAM) approach to characterize the urban acoustic environment; a case comparison of urban mixed-use and forest. Applied Acoustics 185, 108387.

Lionello, M., Aletta, F., Kang, J., 2020. A systematic review of prediction models for the experience of urban soundscapes. Applied Acoustics 170, 107479.

Ma, K.W., Mak, C.M., Wong, H.M., 2021. Effects of environmental sound quality on soundscape preference in a public urban space. Applied Acoustics 171, 107570.

Montoya-Belmonte, J., Navarro, J.M., 2020. Long-Term Temporal Analysis of Psychoacoustic Parameters of the Acoustic Environment in a University Campus Using a Wireless Acoustic Sensor Network. Sustainability 12, 7406.

Newman, M., 2018. Networks. Oxford university press.

Nichols, S.M., Bradley, D.L., 2019. Use of noise correlation matrices to interpret ocean ambient noise. The Journal of the Acoustical Society of America 145, 2337-2349.

Orban, E., McDonald, K., Sutcliffe, R., Hoffmann, B., Fuks, K.B., Dragano, N., Viehmann, A., Erbel, R., Jöckel, K.-H., Pundt, N., 2016. Residential road traffic noise and high depressive symptoms after five years of follow-up: results from the Heinz Nixdorf recall study. Environmental Health Perspectives 124, 578-585.

Peris, E., Blanes, N., Fons, J., Maza, M.S.d.l., Ramos, M.J., Domingues, F., Biala, K., Peterlin, M., Ganzleben, C., Adams, M., 2019. Environmental noise in Europe - 2020. EEA, Luxembourg.

Phillips, Y.F., Towsey, M., Roe, P., 2018. Revealing the ecological content of long-duration audio-recordings of the environment through clustering and visualisation. PLOS ONE 13, e0193345.

Pieretti, N., Duarte, M.H.L., Sousa-Lima, R.S., Rodrigues, M., Young, R.J., Farina, A., 2015. Determining Temporal Sampling Schemes for Passive Acoustic Studies in Different Tropical Ecosystems. Tropical Conservation Science 8, 215-234.

Pijanowski, B.C., Farina, A., Gage, S.H., Dumyahn, S.L., Krause, B.L., 2011. What is soundscape ecology? An introduction and overview of an emerging new science. Landscape Ecology 26, 1213-1232.

Raimbault, M., Lavandier, C., Bérengier, M., 2003. Ambient sound assessment of urban environments: field studies in two French cities. Applied Acoustics 64, 1241-1256.

Regionalverband Ruhr, 2020. Flächennutzungskartierung. Daten für die Stadt- und Regionalplanung. https://www.rvr.ruhr/daten-digitales/geodaten/flaechennutzungskartierung/ (last accessed on 01.05.2023).

Rehan, R.M., 2016. The phonic identity of the city urban soundscape for sustainable spaces. HBRC journal 12, 337-349.

Scott, D.W., Sheather, S.J., 1985. Kernel density estimation with binned data. Communications in Statistics - Theory and Methods 14, 1353-1359.

Sethi, S.S., Ewers, R.M., Jones, N.S., Sleutel, J., Shabrani, A., Zulkifli, N., Picinali, L., 2022. Soundscapes predict species occurrence in tropical forests. Oikos 2022, e08525.

Shannon, C.E., 1948. A mathematical theory of communication. The Bell System Technical Journal 27, 379-423.

Stam, C.J., Reijneveld, J.C., 2007. Graph theoretical analysis of complex networks in the brain. Nonlinear Biomedical Physics 1, 3.

Stowell, D., Wood, M.D., Pamuła, H., Stylianou, Y., Glotin, H., 2019. Automatic acoustic detection of birds through deep learning: The first Bird Audio Detection challenge. Methods in Ecology and Evolution 10, 368-380.

Straßenwesen, B.f., 2022. Automatische Dauerzählstellen auf Autobahnen und Bundesstraßen. https://www.bast.de/DE/Verkehrstechnik/Fachthemen/v2-verkehrszaehlung/zaehl_node.html (last accessed on 01.05.2023).

Sueur, J., 2018. Sound analysis and synthesis with R. Springer, Culemborg, Netherlands.

Sueur, J., Farina, A., 2015. Ecoacoustics: the ecological investigation and interpretation of environmental sound. Biosemiotics 8, 493-502.

Toubiana, D., Maruenda, H., 2021. Guidelines for correlation coefficient threshold settings in metabolite correlation networks exemplified on a potato association panel. BMC Bioinformatics 22, 116.

Towsey, M., Zhang, L., Cottman-Fields, M., Wimmer, J., Zhang, J., Roe, P., 2014. Visualization of Long-duration Acoustic Recordings of the Environment. Procedia Computer Science 29, 703-712.

Ulloa, J.S., Aubin, T., Llusia, D., Bouveyron, C., Sueur, J., 2018. Estimating animal acoustic diversity in tropical environments using unsupervised multiresolution analysis. Ecological Indicators 90, 346-355.

van Kempen, E., Devilee, J., Swart, W., van Kamp, I., 2014. Characterizing urban areas with good sound quality: development of a research protocol. Noise Health 16, 380-387.

WHO, 2018. Environmental noise guidelines for the European region. WHO Regional Office for Europe, Copenhagen, Denmark.

Wildlife Acoustics, 2020. Song Meter SM4 Acoustic Recorder. https://www.wildlifeacoustics.com/products/song-meter-sm4 (last accessed on 01.05.2023).

Yang, W., Kang, J., 2005. Acoustic comfort evaluation in urban open public spaces. Applied Acoustics 66, 211-229.